scientific reports

Check for updates

OPEN

Protein disulfide isomerase integrates toll-like receptor 4 and P2X7 receptor signaling pathways during lipopolysaccharide-induced neuroinflammation

Ji-Eun Kim[1,2]✉, Su Hyeon Wang[1,2], Duk-Shin Lee[1,2] & Tae-Hyun Kim[1,2]

P2X7 receptor (P2X7R) augments lipopolysaccharide (LPS)-toll-like receptor 4 (TLR4)-mediated neuroinflammation. These roles of P2X7R in neuroinflammation are relevant to nitrosative stress through nuclear factor-κB (NF-κB)-inducible nitric oxide synthase (iNOS) pathway, while the underlying mechanisms are largely unknown. In the present study, we investigated whether protein disulfide isomerase (PDI) is involved in the integration of TLR4-P2X7R functions in response to LPS in vivo. The present study showed that LPS elicited NF-κB-mediated PDI upregulation, iNOS induction and *S*-nitrosylated PDI (SNO-PDI) level, independent of *S*-nitrosylation of NF-κB p65 subunit, in *P2X7R*$^{+/+}$ mice more than *P2X7R*$^{-/-}$ mice. SN50 (an NF-κB inhibitor) effectively diminished LPS-induced PDI upregulation in both *P2X7R*$^{+/+}$ and *P2X7R*$^{-/-}$ mice. *PDI* knockdown attenuated LPS-induced p65 S276 phosphorylation and iNOS induction in both strains. Of interest, *S*-nitroso-*N*-acetyl-DL-penicillamine (SNAP, a NO donor) increased SNO-PDI level, surface P2X7R expression and p65 S276 phosphorylation in *P2X7R*$^{+/+}$ mice under physiological condition. In *P2X7R*$^{-/-}$ mice, SNAP was less effective on NF-κB S276 phosphorylation, although SNO-PDI level was similar to that in *P2X7R*$^{+/+}$ mice. Taken together, the present data demonstrate that PDI may be an intermediator to integrate TLR4- and P2X7R-mediated signaling pathways in a positive feedback loop, which would exert NF-κB-iNOS-mediated nitrosative stress during LPS-induced neuroinflammation.

Keywords Astrocyte, LPS, Microglia, Nitrosative stress, S-nitrosylation, SN50, SNAP, TLR4-P2X7R interaction

In various neurological diseases, neuroinflammation aggravates the brain lesion by generating reactive oxygen species, proteolytic enzymes and proinflammatory cytokines. Therefore, the inhibition of neuroinflammation is one of the therapeutic interventions for promoting neuroprotection and avoidance of brain injury. P2X7 receptor (P2X7R), an ATP-gated nonselective cationic channel, has attracted much attention as the modulator of inflammatory pathways in the brain by regulating proinflammatory signaling molecules including inducible nitric oxide synthase (iNOS) and nuclear factor-κB (NF-κB)[1–4]. P2X7R augments lipopolysaccharide (LPS)-toll-like receptor 4 (TLR4)-mediated neuroinflammation[4,5]. These roles of P2X7R in neuroinflammation are relevant to iNOS-induced nitrosative stress in a positive feedback manner[4,5], while intermediators have been elusive.

Protein disulfide isomerase (PDI) plays an important role as a chaperone in endoplasmic reticulum (ER), which catalyzes formation, reduction and isomerization of disulfide bonds in proteins. PDI has an oxidoreductase activity regulating redox states of cell surface receptors, and also acts as a donor of nitric oxide (NO) and a denitrosylase modulating *S*-nitrosylation of cytosolic proteins (an oxidative modification of a thiol (-SH) converting to a nitrosothiol (-SNO) between NO and a redox-reactive cysteine)[6–10]. Interestingly, PDI regulates a P2X7R-dependent activation of prothrombotic tissue factor (TF) that is a coagulation cofactor/receptor expressed in the vessel wall[11,12]. Furthermore, PDI exerts the trafficking of P2X7R by modulating dynamic redox status and *S*-nitrosylation of cysteine residues on an extracellular domain forming disulfide bonds, which reinforces microglial activation induced by seizures[13]. PDI also elicits NF-κB p65-serine (S) 276 phosphorylation

[1]Department of Anatomy and Neurobiology, College of Medicine, Hallym University, Chuncheon 24252, Korea. [2]Institute of Epilepsy Research, College of Medicine, Hallym University, Chuncheon 24252, Korea. ✉email: jieunkim@hallym.ac.kr

that enhances its transactivation potentials and microglial activation[13,14]. Therefore, it is likely that PDI would function as a cofactor for many transcription factors affected by P2X7R, suggesting the cooperation between P2X7R and PDI in the pathogenesis of NF-κB-mediated neuroinflammation. However, there are controversial in the literatures concerning this: (1) LPS lowers PDI level caused by oxidative stress-induced degradation[15], while it enhances PDI induction[16,17]. (2) PDI suppresses LPS-induced NF-κB transactivation without affecting its DNA-binding activity and phosphorylation[18,19], whereas it elicits expressions of proinflammatory factors by increasing NF-κB phosphorylation[20–22]. (3) Reduction of a disulfide bond on NF-κB by thioredoxin (TRX) increases its DNA binding activity[23,24], which is suppressed by PDI in a dose-dependent manner[18]. With respect to these previous reports, notable questions have been raised (1) whether PDI is a mediator for P2X7R-NF-κB-iNOS signal pathway generating LPS-induced nitrosative stress, (2) the *S*-nitrosylation of PDI distinctly modulates NF-κB transcription activity in response to LPS, which would contribute to the discrepancies in previous studies, and (3) *P2X7R* ablation changes the action of thiol-modifying oxidoreductase activity of PDI under LPS-induced inflammatory condition. Considering the roles of P2X7R and nitrosative stress in neuroinflammation[1–5], it is noteworthy elucidating these questions to understand the novel mechanism of neuroinflammation, which would provide a strategy for inflammation-related neurological diseases.

Here, we demonstrate that LPS elicited NF-κB-mediated PDI upregulation, iNOS induction and *S*-nitrosylated PDI (SNO-PDI) level, independent of *S*-nitrosylation of NF-κB p65 subunit, in $P2X7R^{+/+}$ mice more than $P2X7R^{-/-}$ mice. SN50 (an NF-κB inhibitor) effectively diminished LPS-induced PDI upregulation in both $P2X7R^{+/+}$ and $P2X7R^{-/-}$ mice. *PDI* knockdown attenuated LPS-induced p65 S276 phosphorylation and iNOS induction in both strains. Furthermore, *S*-nitroso-*N*-acetyl-DL-penicillamine (SNAP, a NO donor) increased SNO-PDI level, surface P2X7R expression and p65 S276 phosphorylation in $P2X7R^{+/+}$ mice under physiological condition. In $P2X7R^{-/-}$ mice, SNAP was less effective on NF-κB S276 phosphorylation, although SNO-PDI level was similar to that in $P2X7R^{+/+}$ mice. These findings indicate that PDI may play an important role in a positive feedback loop of TLR4 and P2X7R interactions to regulate NF-κB activation following LPS treatment.

Results

P2X7R ablation inhibits PDI upregulation following LPS treatment

First, we explored whether *P2X7R* deletion affects PDI expression in the mouse hippocampus following LPS treatment. *P2X7R* deletion did not affect total PDI protein level in the hippocampus under physiological condition (Fig. 1A). LPS increased total PDI protein level in the hippocampus of $P2X7R^{+/+}$ mice ($\chi^2_{(3)} = 22.163$, $p < 0.001$, Kruskal–Wallis with Dunn-Bonferroni *post-hoc* test, $n = 7$, respectively, Fig. 1A and Supplementary Fig. 1), accompanied by microglial activation (Fig. 1B). *P2X7R* deletion attenuated LPS-induced microglial activation (Fig. 1B) and PDI upregulation in the hippocampus ($p = 0.027$, Kruskal–Wallis with Dunn-Bonferroni *post-hoc* test, $n = 7$, respectively, Fig. 1A).

Immunofluorescent study reveals that LPS increased PDI levels in microglia and astrocytes in $P2X7R^{+/+}$ mice more than $P2X7R^{-/-}$ mice ($z = 2.875$, $p = 0.004$, $n = 7$, respectively, Mann–Whitney test; Fig. 1C–E). Consistent with a previous study[4], *P2X7R* ablation inhibited LPS-induced microglial activation ($z = 3.006$, $p = 0.003$, $n = 7$, respectively, Mann–Whitney test), but not reactive astrogliosis ($z = 0.321$, $p = 0.748$, $n = 7$, respectively, Mann–Whitney test; Fig. 1C–E). These findings indicate that P2X7R may reinforce PDI upregulation in response to LPS, concomitant with microglial activation.

NF-κB activation elicits PDI upregulation in response to LPS in $P2X7R^{+/+}$ and $P2X7R^{-/-}$ mice

NF-κB is known as one of key regulators during LPS-induced inflammatory process. In particular, p65 S276 phosphorylation is required for microglial activation under neuroinflammatory condition[25–27], which is regulated by P2X7R[28]. Therefore, we investigated the changed p65 S276 phosphorylation induced by LPS. *P2X7R* deletion did not alter NF-κB expression and p65 S276 phosphorylation under basal condition (Fig. 2A and Supplementary Fig. 2). LPS increased p65 expression level to 1.56-fold of basal level in $P2X7R^{+/+}$ mice. *P2X7R* deletion attenuated LPS-induced p65 upregulation ($\chi^2_{(3)} = 22.4$, $p < 0.001$, Kruskal–Wallis with Dunn-Bonferroni *post-hoc* test, $n = 7$, respectively, Fig. 2A). p65 S276 phosphorylation was also enhanced in $P2X7R^{+/+}$ mice more than $P2X7R^{-/-}$ mice following LPS treatment ($\chi^2_{(3)} = 20.555$, $p < 0.001$, Kruskal–Wallis with Dunn-Bonferroni *post-hoc* test, $n = 7$, respectively, Fig. 2A). Immunofluorescent study also revealed that *P2X7R* deletion ameliorated LPS-induced p65 S276 phosphorylation ($z = 2.686$, $p = 0.007$, $n = 7$, respectively, Mann–Whitney test; Fig. 2B, C). To investigate further the role of NF-κB activation in LPS-induced PDI upregulation, we also applied SN50 (an NF-κB inhibitor). SN50 effectively diminished LPS-induced PDI upregulation in both strains ($\chi^2_{(3)} = 17.469$, $p = 0.001$, Kruskal–Wallis with Dunn-Bonferroni *post-hoc* test, $n = 7$, respectively, Fig. 2D and Supplementary Fig. 2). These findings indicate that NF-κB may be one of the upstream regulators for PDI upregulation in response to LPS.

PDI knockdown attenuates LPS-induced p65 S276 phosphorylation and iNOS induction in $P2X7R^{+/+}$ mice more than $P2X7R^{-/-}$ mice

In RAW 264.7 cells (a monocyte/macrophage cell line derived from mice), *PDI* overexpression suppresses the NF-κB transcriptional activity induced by LPS treatment[18]. In contrast, *PDI* deletion also inhibits NF-κB activation following LPS treatment[20]. To confirm the role of PDI in LPS-induced NF-κB activation, thus, we investigated the effects of *PDI* siRNA on p65 S276 phosphorylation. *PDI* knockdown effectively inhibited LPS-induced PDI upregulation ($\chi^2_{(3)} = 19.511$, $p < 0.001$, Kruskal–Wallis with Dunn-Bonferroni *post-hoc* test, $n = 7$, respectively, Fig. 3A and Supplementary Fig. 3). As compared to control siRNA, *PDI* knockdown attenuated LPS-induced NF-κB upregulation ($\chi^2_{(3)} = 21.454$, $p < 0.001$, Kruskal–Wallis with Dunn-Bonferroni *post-hoc* test, $n = 7$, respectively, Fig. 3A) and p65 S276 phosphorylation in $P2X7R^{+/+}$ and $P2X7R^{-/-}$ mice ($\chi^2_{(3)} = 19.926$, $p < 0.001$, Kruskal–Wallis with Dunn-Bonferroni *post-hoc* test, $n = 7$, respectively, Fig. 3A and Supplementary Fig. 3).

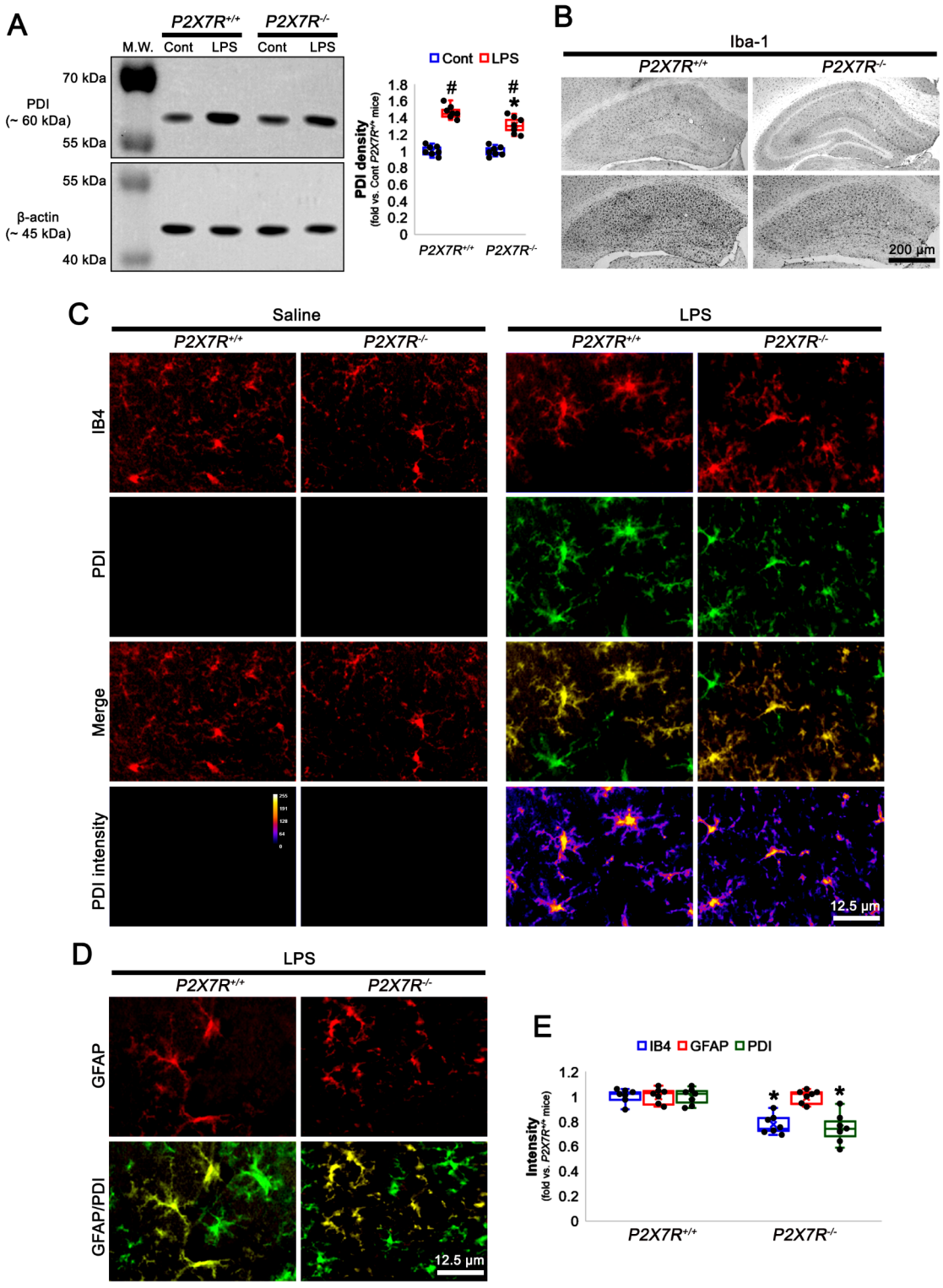

Fig. 1. Effects of *P2X7R* deletion on PDI expression and reactive gliosis in response to LPS. *P2X7R* deletion does not alter PDI expression level in the hippocampus under physiological condition. *P2X7R* ablation attenuates PDI upregulation and microglial (not astroglial) activation following LPS treatment. (**A**) Effects of *P2X7R* deletion on PDI expression in response to LPS. Representative Western blot images for PDI (left panels) and quantification of the effects of *P2X7R* deletion on PDI density (right panel) following LPS treatment ($^{\#}$,$^{*}p < 0.05$ vs. control and $P2X7R^{+/+}$mice, respectively; Kruskal–Wallis test, $n = 7$, respectively). (**B**) Representative photos for Iba-1 positive microglia in the hippocampus following LPS treatment. (**C**, **D**) Representative immunofluorescent images for PDI expression in microglia (**C**) and astrocytes. (**E**) Quantification of the effects of *P2X7R* deletion on IB4 (a microglial marker), GFAP (an astroglial marker) and PDI intensities under post-LPS condition ($^{*}p < 0.05$ vs. $P2X7R^{+/+}$mice, respectively; Mann–Whitney test, $n = 7$, respectively).

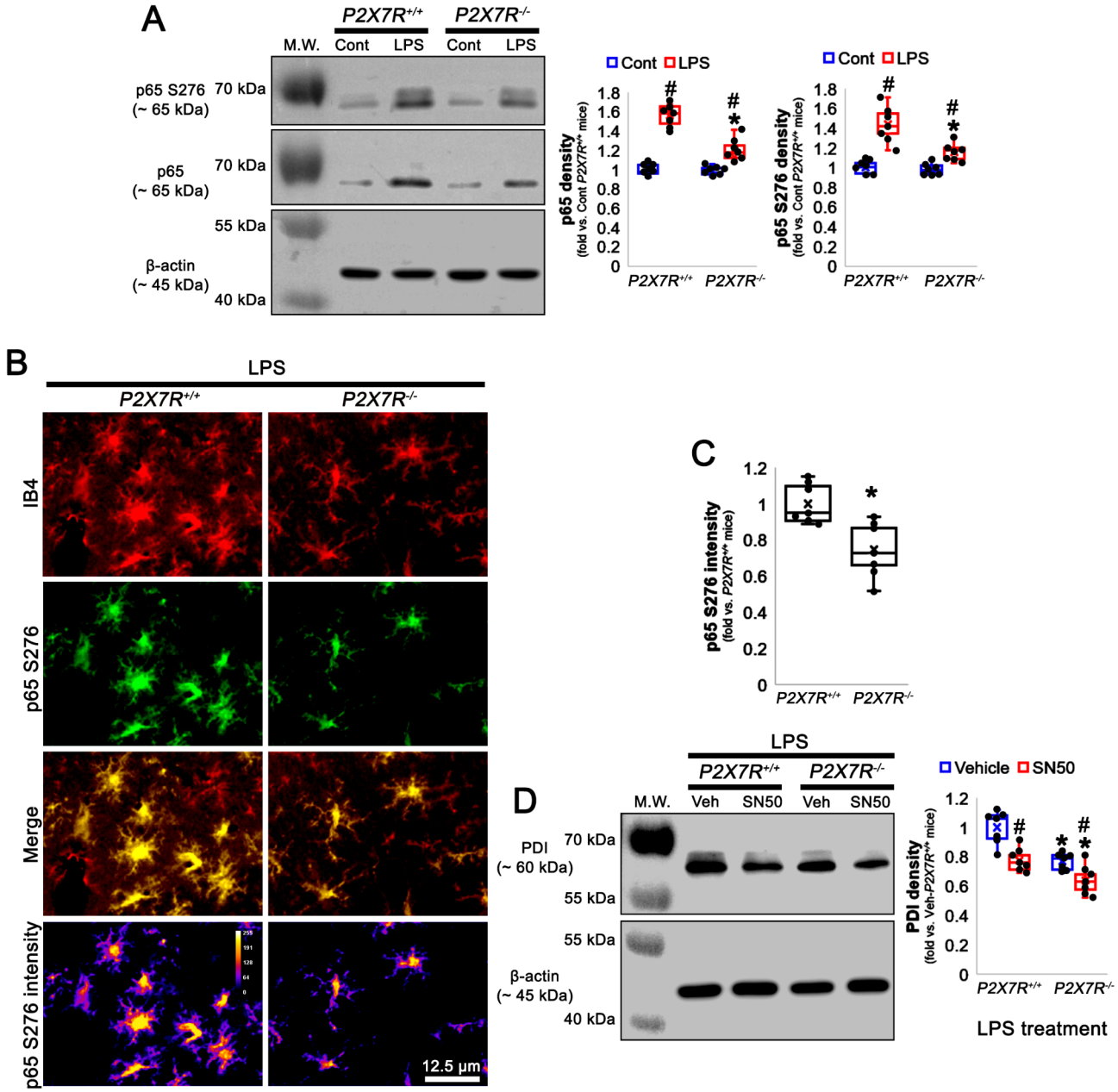

Fig. 2. Effects of P2X7R-mediated NF-κB activation on PDI upregulation in response to LPS. *P2X7R* deletion cannot affect p65 expression and its S276 phosphorylation under basal condition. LPS augments p65 expression and p65 S276 phosphorylation in $P2X7R^{+/+}$ mice. P2X7R deletion attenuates these events. SN50 (a NF-κB inhibitor) ameliorates LPS-induced PDI upregulation in $P2X7R^{+/+}$ and $P2X7R^{-/-}$ mice. (**A**) Effects of *P2X7R* deletion on NF-κB activation in response to LPS. Representative Western blot images for p65 expression and p65 S276 phosphorylation (left panel) and quantification of the effects of *P2X7R* deletion on p65 and p65 S276 densities (right panel) following LPS treatment ($^{\#},^{*}p < 0.05$ vs. control and $P2X7R^{+/+}$mice, respectively; Kruskal–Wallis test, $n = 7$, respectively). (**B**) Representative photos for p65 S276 phosphorylation in microglia under post-LPS condition. (**C**) Quantification of the effects of *P2X7R* deletion on p65 S276 level in microglia under post-LPS condition ($^{*}p < 0.05$ vs. $P2X7R^{+/+}$mice, respectively; Mann–Whitney test, $n = 7$, respectively). (**D**) Effects of SN50 on PDI expression in response to LPS. Representative Western blot images for PDI expression (left panel) and quantification of the effects of SN50 on PDI density (right panel) under post-LPS condition ($^{\#},^{*}p < 0.05$ vs. vehicle and $P2X7R^{+/+}$mice, respectively; Kruskal–Wallis test, $n = 7$, respectively).

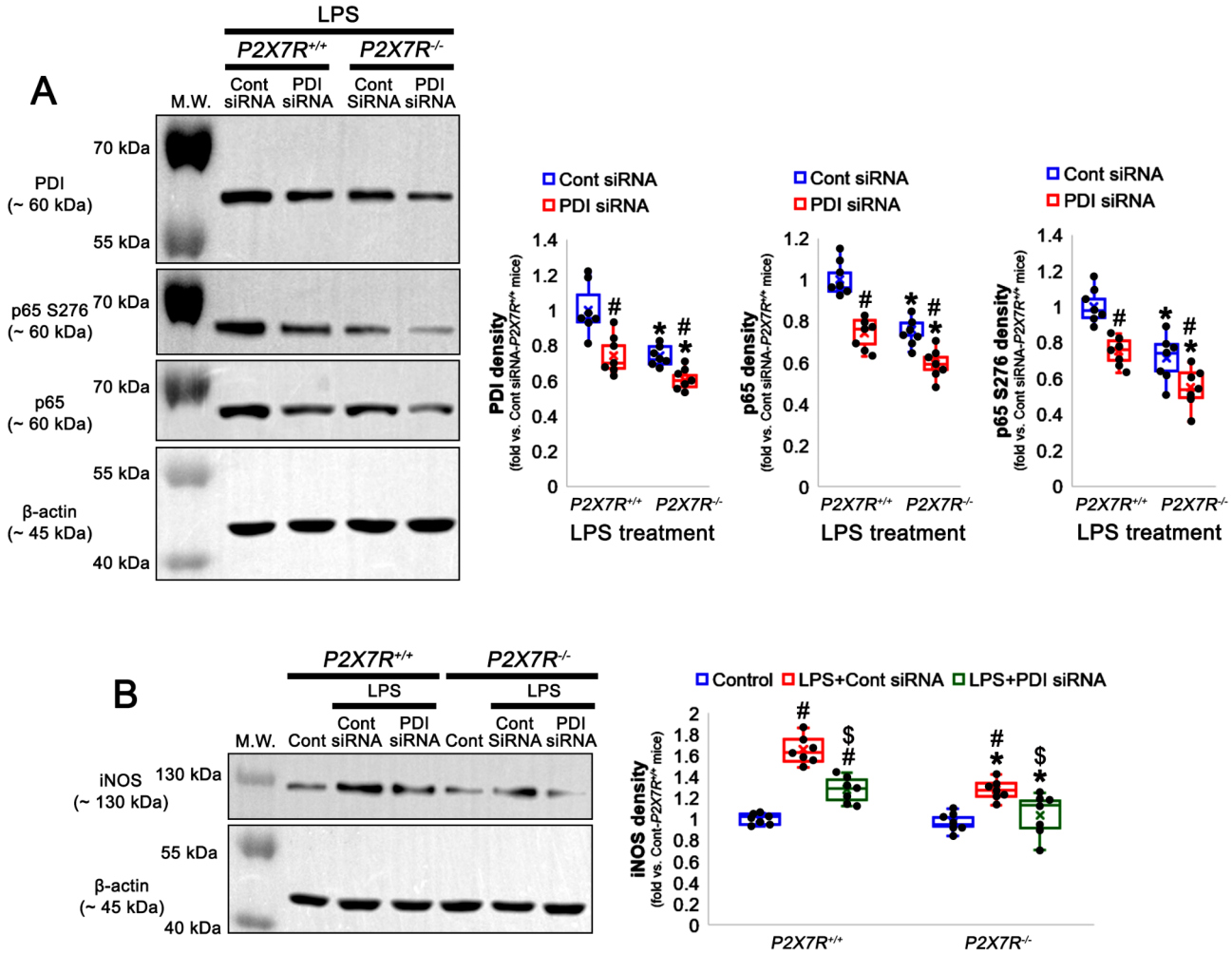

Fig. 3. Roles of PDI in NF-κB activation iNOS induction in response to LPS. *P2X7R* deletion ameliorates PDI upregulation, NF-κB activation and iNOS induction in response to LPS. *PDI* knockdown effectively inhibits LPS-induced PDI upregulation and attenuates LPS-induced NF-κB activation and iNOS induction in $P2X7R^{+/+}$ and $P2X7R^{-/-}$ mice. (**A**) Effects of *PDI* knockdown on NF-κB activation under post-LPS condition. Representative Western blot images for PDI, p65 and p65 S276 levels (left panel) and quantification of the effects of *PDI* knockdown on PDI, p65 and p65 S276 densities (right panel) under post-LPS condition ($^{\#}$,$^{*}p < 0.05$ vs. control siRNA and $P2X7R^{+/+}$mice, respectively; Kruskal–Wallis test, $n = 7$, respectively). (**B**) Effects of *PDI* knockdown on iNOS induction in response to LPS. Representative Western blot images for iNOS level (left panel) and quantification of the effects of *PDI* knockdown on iNOS density (right panel) following LPS treatment ($^{\#}$,$^{*}p < 0.05$ vs. control siRNA and $P2X7R^{+/+}$mice, respectively; Kruskal–Wallis test, $n = 7$, respectively).

These findings indicate that NF-κB and PDI may reciprocally regulate each other following LPS treatment, and P2X7R may intervene in this interaction.

LPS-induced NF-κB activation leads to iNOS induction, which evokes nitrosative stress[29–31]. To elucidate the role of PDI in NF-κB-mediated iNOS induction, we evaluated the effect of *PDI* knockdown on iNOS induction following LPS treatment. Under physiological conditions, these was no difference in iNOS protein level between $P2X7R^{+/+}$ and $P2X7R^{-/-}$ mice. LPS increased iNOS expression in $P2X7R^{+/+}$ mice more than $P2X7R^{-/-}$ mice ($p = 0.017$, Kruskal–Wallis with Dunn-Bonferroni *post-hoc* test, $n = 7$, respectively, Fig. 3B and Supplementary Fig. 3). *PDI* siRNA attenuated LPS-induced iNOS upregulation in both strains ($\chi^2_{(5)} = 32.078$, $p < 0.001$, Kruskal–Wallis with Dunn-Bonferroni *post-hoc* test, $n = 7$, respectively, Fig. 3B). These findings indicate that P2X7R may amplify PDI-mediated argumentation of NF-κB-iNOS activation in response to LPS.

P2X7R-mediated NF-κB activation upregulates PDI expression without affecting the yield of *S*-nitrosylation of PDI following LPS treatment

P2X7R also regulates iNOS-mediated nitrosative stress[2–5]. Indeed, *P2X7R* ablation reduces SNO-cysteine production in microglia and astrocytes under physiological and LPS-induced inflammatory conditions[4]. In the present study, furthermore, *P2X7R* ablation inhibited LPS-induced iNOS induction. Since *S*-nitrosylation of PDI

determines its enzyme properties as a denitrosylase or a NO transporter[6,32], we investigated whether P2X7R-mediated NF-κB activation affects *S*-nitrosylation of PDI following LPS treatment.

P2X7R ablation did not affect basal PDI level. However, *P2X7R* ablation attenuated the increased PDI expression in response to LPS. SN50 ameliorated LPS-induced PDI upregulation in both strains ($\chi^2_{(5)} = 35.958$, $p < 0.001$, Kruskal–Wallis with Dunn-Bonferroni *post-hoc* test, $n = 7$, respectively, Fig. 4A, B and Supplementary Fig. 4). Under physiological condition, SNO-PDI level in $P2X7R^{-/-}$ mice was lower than that in $P2X7R^{+/+}$ mice. LPS increased SNO-PDI level in $P2X7R^{+/+}$ mice more than $P2X7R^{-/-}$ mice, which were attenuated by SN50 ($\chi^2_{(5)} = 36.462$, $p < 0.001$, Kruskal–Wallis with Dunn-Bonferroni *post-hoc* test, $n = 7$, respectively, Fig. 4A, C). Under physiological condition, SNO-PDI ratio (SNO-PDI/total PDI ratio) in $P2X7R^{-/-}$ mice was lower than that in $P2X7R^{+/+}$ mice ($p = 0.001$, Kruskal–Wallis with Dunn-Bonferroni *post-hoc* test, $n = 7$, respectively, Fig. 4A, D). However, LPS increased SNO-PDI ratio in $P2X7R^{-/-}$ mice ($p = 0.032$, Kruskal–Wallis with Dunn-Bonferroni *post-hoc* test, $n = 7$, respectively), but not in $P2X7R^{+/+}$ mice (Fig. 4A, D). SN50 did not affect SNO-PDI ratio in both strains following LPS treatment (Fig. 4A, D). These findings indicate that P2X7R may augment LPS-induced neuroinflammation by enhancing basal SNO-PDI ratio and NF-κB-mediated PDI upregulation, although both P2X7R and NF-κB pathways may not affect the yield of *S*-nitrosylation of PDI following LPS treatment.

P2X7R and PDI do not affect SNO-p65 level following LPS treatment

NF-κB p65 subunit is constitutively *S*-nitrosylated on cysteine 38 residue, which inhibits NF-κB transcriptional activity[33–35]. LPS exerts a decrease in SNO-p65 levels concomitant with NF-κB activation in initiation of the inflammatory responses[36]. Therefore, *S*-nitrosylation of p65 is proposed as a negative feedback mechanism to iNOS induction in response to LPS. Since the present study revealed that LPS increased SNO-PDI level, we validated whether PDI regulates NF-κB activation by affecting *S*-nitrosylation of p65 subunit following LPS treatment.

P2X7R deletion did not alter basal p65 level. LPS increased p65 expression level in $P2X7R^{+/+}$ mice more than $P2X7R^{-/-}$ mice, which were ameliorated by *PDI* siRNA ($\chi^2_{(5)} = 37.425$, $p < 0.001$, Kruskal–Wallis with Dunn-Bonferroni *post-hoc* test, $n = 7$, respectively, Fig. 5A, B and Supplementary Fig. 5). Under physiological condition, there was no difference in SNO-p65 level between $P2X7R^{+/+}$ and $P2X7R^{-/-}$ mice. LPS reduced SNO-p65 levels in both strains, which were unaffected by *PDI* knockdown ($\chi^2_{(5)} = 27.701$, $p < 0.001$, Kruskal–Wallis with Dunn-Bonferroni *post-hoc* test, $n = 7$, respectively, Fig. 5A, C). There was no difference in SNO-p65

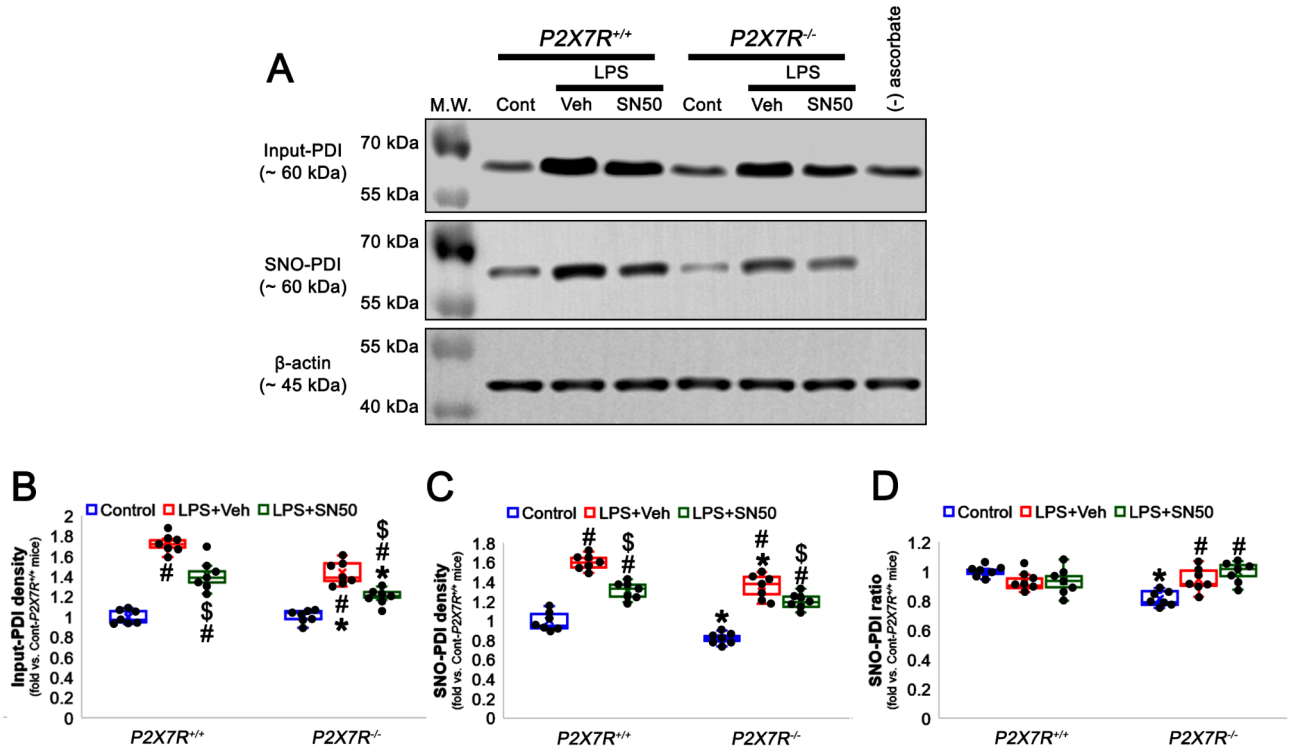

Fig. 4. The roles of P2X7R-mediated NF-κB activation in PDI expression and its *S*-nitrosylation following LPS treatment. *P2X7R* ablation cannot affect basal PDI level, but decreases *S*-nitrosylated (SNO-) PDI level under physiological condition. *P2X7R* deletion ameliorates LPS-induced PDI upregulation and SNO-PDI level, which are ameliorated by SN50 in $P2X7R^{+/+}$ and $P2X7R^{-/-}$ mice. However, LPS increases SNO-PDI ratio only in $P2X7R^{-/-}$ mice, which is unaffected by SN50. (**A**) Representative Western blot images for PDI and SNO-PDI levels following LPS treatment. (**B**–**D**) Quantification of the effects of SN50 on PDI upregulation (**B**), SNO-PDI level (**C**) and SNO-PDI ratio (**D**) in response to LPS ($^{\#,\star,\$}p < 0.05$ vs. control, $P2X7R^{+/+}$mice and vehicle, respectively; Kruskal–Wallis test, $n = 7$, respectively).

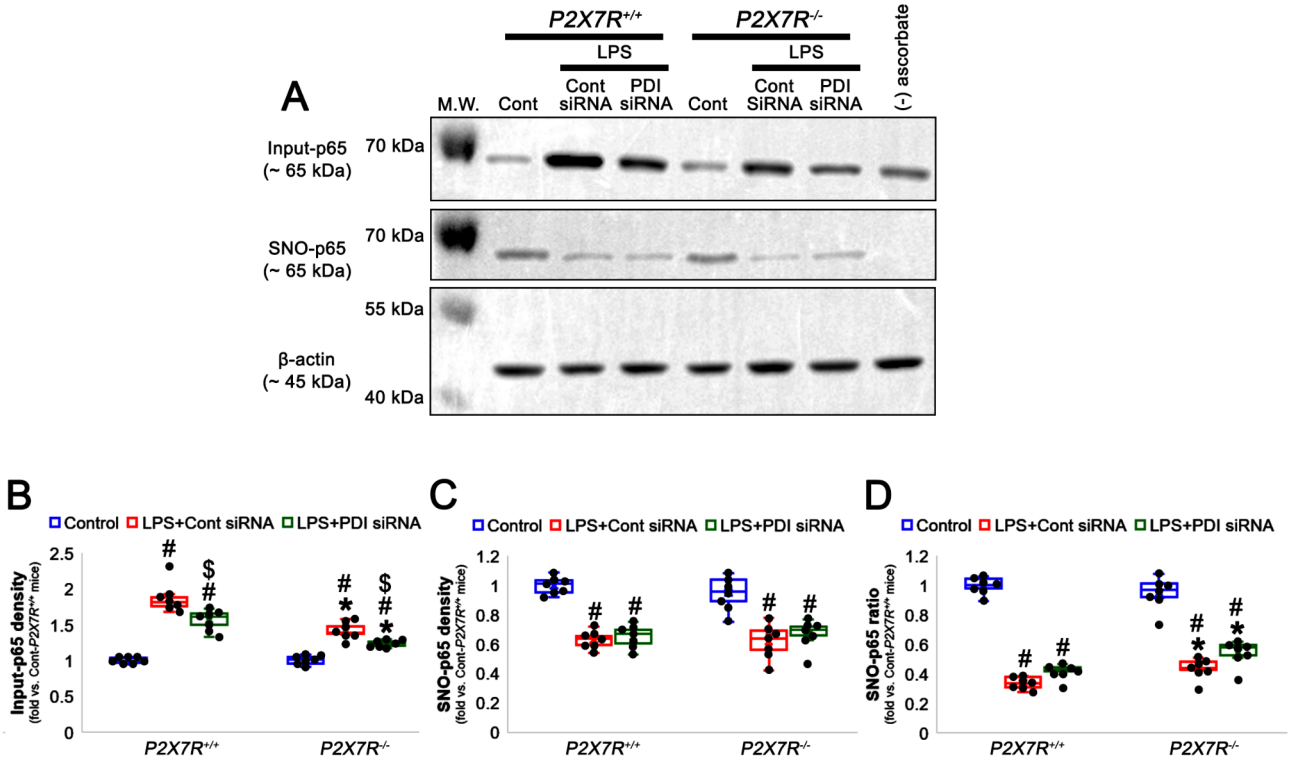

Fig. 5. The effects of *PDI* knockdown on *S*-nitrosylation of p65 following LPS treatment. *P2X7R* ablation cannot affect basal p65 and *S*-nitrosylated (SNO-) p65 levels under physiological condition. LPS increases p65 expression, but reduces SNO-p65 level and its ratio. *P2X7R* deletion ameliorates LPS-induced p65 upregulation without affecting SNO-p65 level. Thus, *P2X7R* deletion mitigates LPS-induced downregulation of SNO-p65 ratio. *PDI* knockdown attenuates LPS-induced p65 upregulation in $P2X7R^{+/+}$ and $P2X7R^{-/-}$ mice without altering SNO-p65 level and SNO-p65 ratio. (**A**) Representative Western blot images for p65 and SNO-p65 levels following LPS treatment. (**B**–**D**) Quantification of the effects of *PDI* knockdown on p65 upregulation (B), SNO-p65 level (**C**) and SNO-p65 ratio (**D**) in response to LPS ($^{\#,\star,\$}p < 0.05$ vs. control, $P2X7R^{+/+}$mice and control siRNA, respectively; Kruskal–Wallis test, $n = 7$, respectively).

ratio (SNO-p65/total p65 ratio) between $P2X7R^{+/+}$ and $P2X7R^{-/-}$ mice under physiological condition (Fig. 5A, D). LPS also diminished SNO-p65 ratio in both strains, which was unaffected by *PDI* knockdown (Fig. 5A, D), although *P2X7R* deletion mitigated the reduced SNO-p65 ratio following LPS treatment ($\chi^2_{(5)} = 34.112$, $p < 0.001$, Kruskal–Wallis with Dunn-Bonferroni *post-hoc* test, $n = 7$, respectively, Fig. 5A, D). These findings indicate that P2X7R may decrease LPS-induced SNO-p65 ratio, independent of PDI, and suggest that PDI may regulate the progress of LPS-induced neuroinflammation rather than initiation.

SNO-PDI augments the integration of P2X7R-NF-κB signaling axis following LPS treatment

PDI-mediated *S*-nitrosylation enhances surface P2X7R expression following status epilepticus (SE)[13]. Furthermore, SNAP (a NO donor) activates microglia by inducing nuclear p65 translocation[37]. Therefore, it is likely that SNO-PDI may play an important role in a positive feedback loop of P2X7R-NF-κB interaction. To confirm this, we applied SNAP to confirm this hypothesis.

Under physiological condition, SNAP augmented IB4 signal ($\chi^2_{(3)} = 22.934$, $p < 0.001$, Kruskal–Wallis with Dunn-Bonferroni *post-hoc* test, $n = 7$, respectively, Fig. 6A, B) and microglial p65 S276 phosphorylation ($\chi^2_{(3)} = 22.908$, $p < 0.001$, Kruskal–Wallis with Dunn-Bonferroni *post-hoc* test, $n = 7$, respectively, Fig. 6A, C) in $P2X7R^{+/+}$ mice more than $P2X7R^{-/-}$ mice, indicating microglial activation. SNAP also similarly increased total PDI ($\chi^2_{(3)} = 20.317$, $p < 0.001$, Kruskal–Wallis with Dunn-Bonferroni *post-hoc* test, $n = 7$, respectively, Fig. 7A, B and Supplementary Fig. 6) and SNO-PDI levels ($\chi^2_{(3)} = 22.852$, $p < 0.001$, Kruskal–Wallis with Dunn-Bonferroni *post-hoc* test, $n = 7$, respectively, Fig. 7A, C) in $P2X7R^{+/+}$ and $P2X7R^{-/-}$ mice. Similar to the case of LPS treatment, SNAP increased SNO-PDI ratio in $P2X7R^{-/-}$ mice, but not in $P2X7R^{+/+}$ mice ($\chi^2_{(3)} = 16.588$, $p < 0.001$, Kruskal–Wallis with Dunn-Bonferroni *post-hoc* test, $n = 7$, respectively, Fig. 7A, D). Although SNAP did not affect total- and SNO-p65 levels in both strains (Fig. 7A, E, F), it enhanced p65 S276 phosphorylation in $P2X7R^{+/+}$ mice more than $P2X7R^{-/-}$ mice ($\chi^2_{(3)} = 22.901$, $p < 0.001$, Kruskal–Wallis with Dunn-Bonferroni *post-hoc* test, $n = 7$, respectively, Fig. 7A, G). In $P2X7R^{+/+}$ mice, SNAP enhanced P2X7R expression ($\chi^2_{(3)} = 25.719$, $p < 0.001$, Kruskal–Wallis with Dunn-Bonferroni *post-hoc* test, $n = 7$, respectively, Fig. 7A, H), SNO-P2X7R level ($\chi^2_{(3)} = 26.055$, $p < 0.001$, Kruskal–Wallis with Dunn-Bonferroni *post-hoc* test, $n = 7$, respectively, Fig. 7A, I) and SNO-P2X7R ratio ($\chi^2_{(3)} = 26.601$, $p < 0.001$, Kruskal–Wallis with Dunn-Bonferroni *post-hoc* test, $n = 7$, respectively, Fig. 7A, J), concomitant with the increased surface P2X7R expression ($\chi^2_{(3)} = 25.831$, $p < 0.001$, Kruskal–Wallis with Dunn-

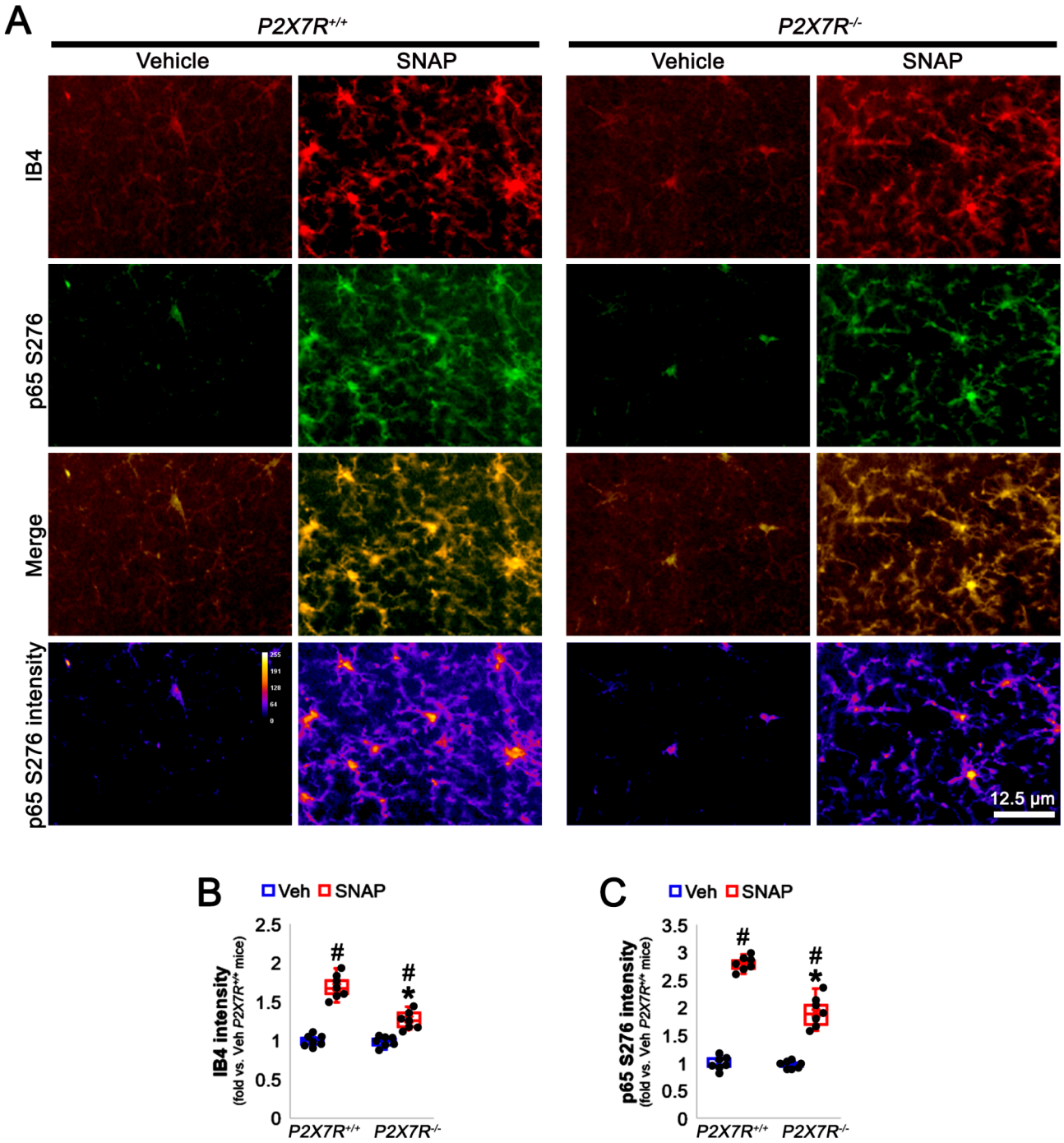

Fig. 6. The effects of NO on microglial activation and p65 S276 phosphorylation under physiological condition. SNAP (a NO donor) leads to microglial activation and p65 phosphorylation under physiological condition, which are attenuated by *P2X7R* deletion. (**A**) Representative photos for p65 S276 phosphorylation in microglia following SNAP treatment. (**B**–**C**) Quantification of the effects of SNAP on IB4 (a microglial marker, **B**) and p65 S276 intensities (**C**; $^{\#,*}p < 0.05$ vs. vehicle and $P2X7R^{+/+}$mice, respectively; Kruskal–Wallis test, $n = 7$, respectively).

Bonferroni *post-hoc* test, $n = 7$, respectively, Fig. 7A, K). Taken together, our findings indicate that SNAP-induced *S*-nitrosylation of PDI may activate NF-κB, which may be elicited by P2X7R in a positive feedback manner.

Discussion

TLR4-NF-κB-iNOS signaling pathway plays an important role in LPS-induced inflammatory processes[29,38]. Furthermore, oxidized ATP (OxATP, an irreversible P2X7R inhibitor) attenuates a NF-κB binding activity, iNOS expression and NO production in response to various stimuli including LPS[39,40]. These reports indicate

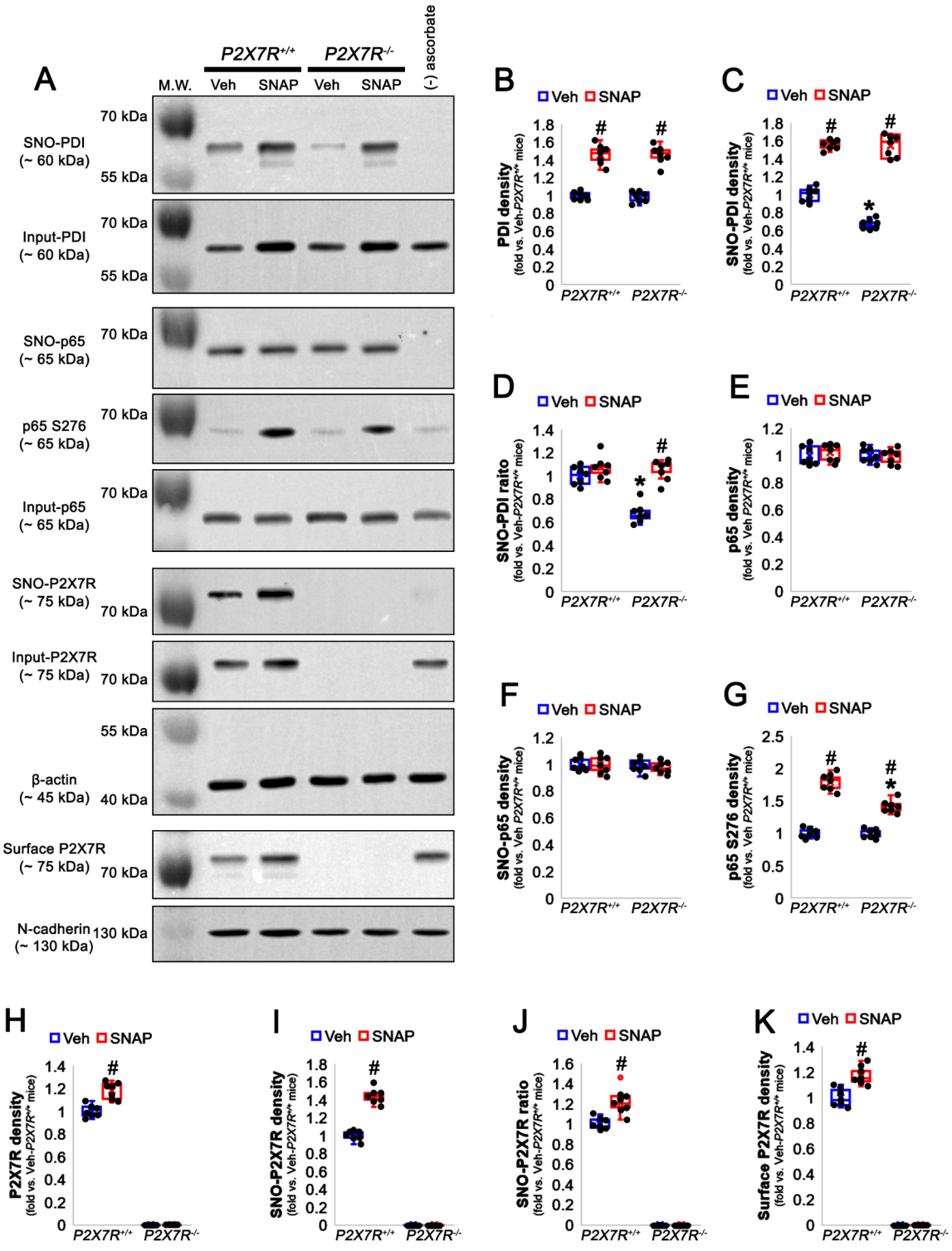

Fig. 7. The effects of SNAP on expression and *S*-nitrosylation of PDI, p65 and P2X7R, and surface P2X7R expression under physiological condition. SNAP upregulates PDI expression and *S*-nitrosylated (SNO-) PDI level, which are unaffected by *P2X7R* deletion. SNAP augments p65 S276 phosphorylation in $P2X7R^{+/+}$ and $P2X7R^{-/-}$ mice without altering p65 and SNO-p65 densities. In addition, SNAP increases total and surface P2X7R expressions, concomitant with enhanced *S*-nitrosylation of P2X7R in $P2X7R^{+/+}$ mice. (**A**) Representative images for expression and *S*-nitrosylation of PDI, p65 and P2X7R, and surface P2X7R expression following SNAP treatment. (**B**–**K**) Quantification of the effects of SNAP on PDI, SNO-PDI, p65, SNO-p65, p65 S276, P2X7R, SNO-P2X7R and surface P2X7R levels ($^{\#,*}p < 0.05$ vs. vehicle and $P2X7R^{+/+}$ mice, respectively; Kruskal–Wallis test, $n = 7$, respectively).

that P2X7R itself modulates NF-κB activity, independent of TLR4. After exposure to LPS, interestingly, P2X7R contributes microglial hyperactivity, which augments NF-κB-mediated iNOS expression and NO production[41–43]. Therefore, we hypothesized that TLR4 and P2X7R may compose a positive feedback loop in the mouse hippocampus during inflammatory processes, which would activate NF-κB-iNOS signaling pathway in response to LPS in vivo. Considering PDI-mediated trafficking of P2X7R and p65 S276 phosphorylation[13], it is likely that PDI may act as an intermediator of this TLR4-P2X7R interaction by regulating NF-κB activity after LPS stimulation. The present data reveal that *S*-nitrosylation of PDI contributes LPS-induced NF-κB activation, which was attenuated by *P2X7R* deletion. Thus, these findings suggest that PDI may integrate TLR4- and P2X7R-mediated signaling pathways during inflammation (Fig. 8).

PDI is an oxidoreductase in the ER of all types of cells. Upregulation of PDI is an important part of unfolded protein response (UPR)[44]. LPS activates the NF-κB pathway and enhances PDI induction[16,17], which elicits expressions of proinflammatory factors including iNOS[20–22,45]. Compatible with these reports, the present data show that LPS led to PDI upregulation, NF-κB S276 phosphorylation and iNOS induction, which was ameliorated by *P2X7R* deletion, *PDI* knockdown and SN50 treatment. Indeed, *PDI* ablation abrogates the inflammatory function of macrophages[20]. Therefore, our findings indicate that P2X7R and PDI may contribute to NF-κB activation induced by LPS and provide an evidence for the presence of TLR4-NF-κB-PDI-P2X7R-mediated signaling loop that may be activated by LPS in a positive feedback mechanism.

PDI also acts as a denitrosylase as well as a NO donor to regulate *S*-nitrosylation of various target proteins in nuclear envelopes, plasma membranes, mitochondria, and other organelles[6,18,32,46,47]. Therefore, *S*-nitrosylation changes the properties of PDI from chaperone/isomerase/denitrosylase to a NO transporter[6–10]. In the present study, SNO-PDI level and its ratio in $P2X7R^{-/-}$ mice were lower than those in $P2X7R^{+/+}$ mice under physiological condition. LPS increased SNO-PDI level in $P2X7R^{+/+}$ mice more than $P2X7R^{-/-}$ mice, which were attenuated by SN50. However, LPS increased SNO-PDI ratio in $P2X7R^{-/-}$ mice, but not in $P2X7R^{+/+}$ mice, which were unaffected by SN50. These findings indicate that both P2X7R and NF-κB pathways may not alter the yield of *S*-nitrosylation of PDI following LPS treatment. Instead, P2X7R may augment LPS-induced neuroinflammation by enhancing basal SNO-PDI ratio and NF-κB-mediated PDI upregulation.

On the other hand, the present study demonstrates that under physiological condition SNAP increased total PDI level in $P2X7R^{-/-}$ mice similar to that in $P2X7R^{+/+}$ mice. SNAP induces ER stress in microglia[48], which upregulates PDI expression[49]. Therefore, it is unsurprising that SNAP upregulated PDI expression in both strains. Furthermore, SNAP similarly elevated SNO-PDI level in $P2X7R^{+/+}$ and $P2X7R^{-/-}$ mice, although

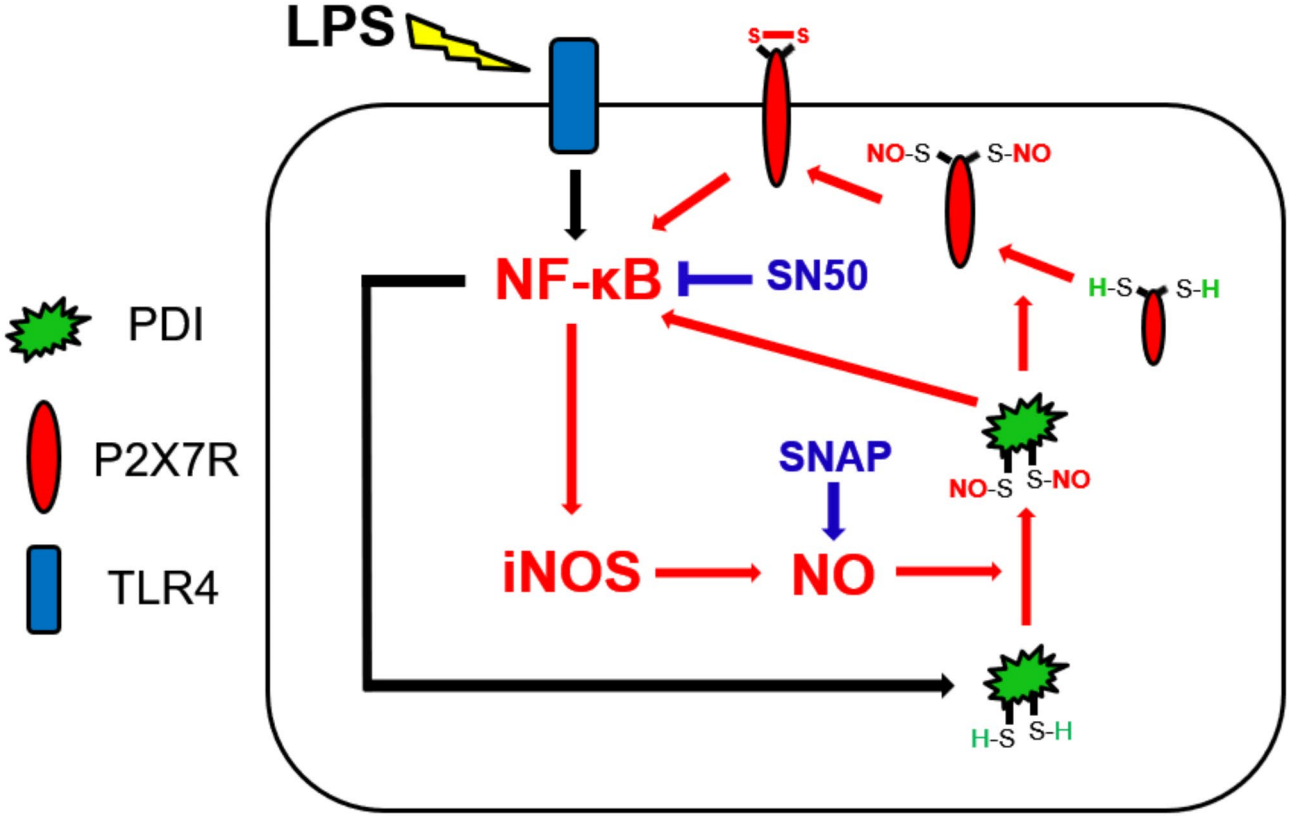

Fig. 8. Scheme of roles of PDI in the integration of TLR4- and P2X7R-mediated signaling pathways during inflammation. LPS-induced TLR4 activation led to NF-κB activation by *S*-nitrosylation and phosphorylation of p65 subunit, which upregulated iNOS and PDI expression in microglia. *S*-nitrosylation of PDI induced by iNOS further augmented NF-κB activation by a direct interaction as well as the enhanced surface P2X7R expression, independent of *S*-nitrosylation of p65.

SNAP increased SNO-PDI ratio only in the *P2X7R*$^{-/-}$ mice, indicating that SNAP induced *S*-nitrosylation of PDI, independent of P2X7R. However, SNAP induced microglial activation in *P2X7R*$^{+/+}$ mice more than *P2X7R*$^{-/-}$ mice. SNAP also elicited p65 S276 phosphorylation in *P2X7R*$^{+/+}$ mice more than *P2X7R*$^{-/-}$ mice. SNAP itself leads to microglial activation through IκB-mediated canonical NF-κB pathway[37]. These data indicate that P2X7R may contribute to SNO-PDI-mediated p65 S276 phosphorylation. Indeed, *PDI* siRNA attenuates microglial activation and the increased P2X7R surface expression induced by SE[13]. Consistent with this report, the present data also reveal that SNAP increased surface P2X7R expression in *P2X7R*$^{+/+}$ mice, accompanied by the enhancement of total- and SNO-P2X7R level. Therefore, our findings indicate that SNO-PDI may control p65 S276 phosphorylation by modulating P2X7R as well as the direct interaction. Taken together with the data obtained from LPS trials, the present data suggest that SNO-PDI may activate NF-κB, which may be elicited by P2X7R in a positive feedback manner.

NF-κB transcriptional activity is negatively regulated by *S*-nitrosylation of p65 subunit[33–35]. Indeed, LPS exerts a decrease in SNO-p65 levels concomitant with NF-κB activation in initiation of the inflammatory responses[36]. Of interest, PDI suppresses TRX that increases DNA binding activity of NF-κB by denitrosylating SNO-p65 and reducing a disulfide bond on NF-κB[18,23,24,50]. Since P2X7R activation augments the DNA-binding activity of NF-κB and iNOS expression following LPS treatment[4,51], it is plausible that P2X7R would reinforce LPS-induced NF-κB transactivation by regulating *S*-nitrosylation of p65 subunit. Unlike PDI, the present data show that no difference in SNO-p65 levels between *P2X7R*$^{+/+}$ and *P2X7R*$^{-/-}$ mice was observed following LPS treatment. The present data also demonstrate that *PDI* knockdown did not affect SNO-p65 level in *P2X7R*$^{+/+}$ and *P2X7R*$^{-/-}$ mice under physiological- and post-LPS conditions. These findings indicate that *S*-nitrosylation of p65 level may be independent of PDI. Furthermore, SNAP did not affect total- and SNO-p65 levels in both strains under physiological condition. NF-κB p65 subunit is constitutively *S*-nitrosylated on cysteine 38 residue, which inhibits NF-κB transcriptional activity[33–35]. LPS elicits a decrease in SNO-p65 level concomitant with NF-κB activation. This process is mediated by TRX. Indeed, inhibition of Trx activity attenuates LPS-induced SNO-p65 denitrosylation and NF-κB activation[36]. Therefore, our findings indicate that TLR4-NF-κB-PDI-P2X7R signaling loop may modulate LPS-induced neuroinflammation, independent of *S*-nitrosylation of p65 subunit.

The present study demonstrates that under physiological condition SNAP increased surface P2X7R expression in *P2X7R*$^{+/+}$ mice, accompanied by the enhancement of total- and SNO-P2X7R level. An extracellular domain of P2X7R has ten cysteine residues forming five intrasubunit disulfide bonds (SS1–SS5)[52], which are needed for its trafficking onto the cell surface[53]. *S*-nitrosylation facilitates disulfide bond formation (oxidation) between cysteine residues[54], which is required for the trafficking of P2X7R[53]. Regarding that PDI exerts the trafficking of P2X7R by modulating dynamic redox status and *S*-nitrosylation of cysteine residues on an extracellular domain forming disulfide bonds[13], SNAP may facilitate surface P2X7R trafficking by increasing SNO-PDI mediated S-nitrosylation of P2X7R.

P2X7R is an ATP-gated nonselective cationic channel. In microglia, P2X7R agonists rapidly activate AMP-activated kinase (AMPK). P2X7R antagonist can abolish agonist-induced AMPK activation, but not that induced by nigericin (K^+ ionophore)[55]. Similarly, P2X7R agonist-induced interleukin-1β (IL-1β) release is inhibited by P2X7R antagonists, while IL-1β release mediated by nigericin is not affected by the addition of P2X receptor antagonists[56]. In addition, LPS-induced macrophage activation is strongly attenuated by the P2X7R antagonists. However, P2X7R antagonists do not affect macrophage stimulation by Ca^{2+} ionophore A23187[57]. Considering these previous reports, it is likely that P2X7R-mediated K^+ efflux and/or Ca^{2+} influx may affect LPS-induced *S*-nitrosylation of PDI. Further studies are needed to validate the effects of ionophore on TLR4-P2X7R interactions in response to LPS-induced nitrosative stress.

In the present study, we provided a novel PDI-mediated positive feedback loop between TLR4- and P2X7R-mediated signaling pathway. LPS-induced TLR4 activation led to NF-κB p65 S276 phosphorylation, which upregulated iNOS and PDI expression in microglia. In turn, iNOS-induced *S*-nitrosylation of PDI further augmented p65 S276 phosphorylation by a direct interaction as well as the enhanced surface P2X7R expression, independent of *S*-nitrosylation of p65. These findings serve as the first comprehensive description indicating that PDI may integrate TLR4- and P2X7R-mediated signaling pathway in a positive feedback manner under neuroinflammatory condition. Therefore, our findings suggest the targeting of PDI may be one of the important therapeutic strategies of neuroinflammation.

Methods

Experimental animals and chemicals

Animal experiments were designed and performed in accordance with the relevant guidelines and regulations. For all the procedures of the study we followed the ARRIVE guidelines. Animal protocols were approved by the Institutional Animal Care and Use Committee of Hallym University (Chuncheon, South Korea, Code number: (#Hallym 2021–30, approval date: May 17, 2021). All reagents were obtained from Sigma-Aldrich unless otherwise indicated. Male C57Bl/6 J (Wild type, *P2X7R*$^{+/+}$) and P2X7R knockout (KO, *P2X7R*$^{-/-}$) mice (60–90-day-old, 25–30 g, The Jackson Laboratory, USA) were used in the present study. Mice were given a diet and water ad libitum under controlled conditions (22 ± 2 °C, 55% ± 5% humidity, and 12-h light/12-h dark cycle).

Surgery, PDI knockdown, drug infusions and LPS treatment

To avoid the limitation of the permeability of the chemicals and siRNA across blood–brain barrier in vivo and maintain their constant concentration in the brain, we applied intracerebroventricular administration. Mice were anesthetized with Isoflurane (3% induction, 1.5–2% for surgery and 1.5% maintenance in a 65:35 mixture of N_2O:O_2). A brain infusion kit 3 (Alzet, USA) was implanted into the right lateral ventricle (1 mm posterior; 1.5 mm lateral; 3.5 mm depth from bregma) and connected to an osmotic pump (1007D, Alzet, USA) containing a vehicle, SN50 (20 μM), *S*-nitroso-*N*-acetyl-D,L-penicillamine (SNAP) (0.1 μM), non-silencing RNA (control

Antigen	Host	Manufacturer (Catalog number)	Dilution
GFAP	Mouse	Millipore (#MAB3402)	1:2000 (IH)
IB4	-	Vector (#B-1205)	1:200 (histochemistry)
Iba-1	Rabbit	Biocare Medical (#CP290)	1:500 (IH)
iNOS	Rabbit	Novus Biologicals (#NB300-605)	1:500 (WB)
N-cadherin	Rabbit	Abcam (ab18203)	1:4000 (WB)
NF-κB p65	Rabbit	Abcam (ab16502)	1:1000 (WB)
NF-κB p65 S276	Rabbit	Abcam (ab106129)	1:100 (IH) 1:1000 (WB)
P2X7R	Rabbit	Alomone labs (#APR-008)	1:500 (WB)
PDI	Rabbit	Proteintech (#11245-1-AP) Cell signaling (#2446)	1:500 (IH) 1:1000 (WB)
β-actin	Mouse	Sigma (#A5316)	1:5000 (WB)

Table 1. Primary antibodies and lectin used in the present study. IH: Immunohistochemistry; WB: Western blot.

siRNA) or mouse *PDI* siRNA (CCUUUGCUAGCGAAUCUCAGAGCC), which were continuously infused over 6-day period[58]. Three days after surgery, mice were given a single dose of LPS (5 mg/kg) or an equal volume of normal saline instead of LPS. Saline-treated mice were used as controls[4].

Western blot

Three days after LPS treatment, animals were sacrificed by decapitation under urethane anesthesia (1.5 g/kg, i.p.). The hippocampus was dissected out and homogenized in lysis buffer (50 mM Tris containing 50 mM 4-(2-hydroxyethyl)-1-piperazineethanesulfonic acid (pH 7.4), ethylene glycol tetraacetic acid (pH 8.0), 0.2% Tergitol type NP-40, 10 mM ethylenediaminetetraacetic acid (pH 8.0), 15 mM sodium pyrophosphate, 100 mM β-glycerophosphate, 50 mM NaF, 150 mM NaCl, 2 mM sodium orthovanadate, 1 mM phenylmethylsulfonyl fluoride, and 1 mM dithiothreitol). Total protein content was measured by BCA protein assay kit. Western blot was performed according to standard procedures (Table 1). The signals were scanned and analyzed by ImageQuant LAS4000 system (GE health). The values of each sample were normalized with the corresponding amount of anti-β-actin (input). The phosphoprotein/total protein ratio was represented as the phosphorylation density[1,4,5,9,10,13,58].

Measurement of *S*-nitrosylation

Modified biotin switch assay was performed with the *S*-nitrosylation Western Blot Kit (ThermoFisher, USA) according to the manufacturer's protocol. Briefly, lysates were reacted with ascorbate in HENS buffer for specific labeling with iodoTMTzero reagents with MMT pretreatment. Protein labeling can be confirmed by Western blot using TMT antibody. Thereafter, TMT-labeled proteins were purified by Anti-TMT Resin, eluted by TMT elusion buffer, and identified by Western blot according to standard procedures as aforementioned. For technical controls, we omitted ascorbate for each sample. The ratio of SNO-protein to total protein was described as *S*-nitrosylation ratio[10,13,58].

Membrane fraction

To analyze membrane expressions of P2X7R, we used subcellular Protein Fractionation Kit for Tissues (Thermo Scientific, USA), according to the manufacturer's instructions. Next, Western blot was performed according to standard procedures[13].

Immunohistochemistry

Three days after LPS injection, animals were anesthetized with urethane anesthesia (1.5 g/kg, i.p.) and perfused transcardially with 4% paraformaldehyde in 0.1 M phosphate buffer (PB, pH 7.4). Brains were post-fixed in the same fixative overnight and then cryoprotected and sectioned at 30 μm with a cryostat. Free-floating sections were washed 3 times in PBS (0.1 M, pH 7.3) and incubated with 3% bovine serum albumin in PBS for 30 min at room temperature. Later, sections were incubated with a cocktail solution containing primary antibodies (Table 1) in PBS containing 0.3% Triton X-100 overnight at room temperature. Thereafter, sections were visualized with appropriate Cy2- and Cy3-conjugated secondary antibodies. Some tissues were incubated in biotinylated IgG and avidin-peroxidase complex and developed in 3,3′-diaminobenzidine in 0.1 M Tris buffer. Immunoreaction was observed using an AxioScope microscope (Carl Zeiss Korea, Seoul, South Korea). To establish the specificity of the immunostaining, a negative control test was carried out with preimmune serum instead of the primary antibody. All experimental procedures in this study were performed under the same conditions and in parallel. To measure fluorescent intensity, five areas/animals (1×10^4 μm^2/area) were randomly selected within the hippocampus (5 sections from each animal, $n = 7$ in each group). Thereafter, the mean intensity of each section was measured by using AxioVision Rel. 4.8 and ImageJ software. Intensity measurements were represented as the number of a 256 grayscale. The intensity of each section was standardized by setting the threshold level (mean background intensity obtained from five image inputs). Fluorescent intensity was performed by two

different investigators who were blind to the classification of tissues. Manipulation of the images was restricted to threshold and brightness adjustments to the whole image[1,4,5,9,10,13].

Statistical analysis

Comparisons of data among groups were analyzed by Mann–Whitney test or Kruskal–Wallis test followed by Dunn-Bonferroni *post-hoc* test. A $p < 0.05$ is considered to be statistically different.

Data availability

The datasets used and/or analyzed during the current study available from the corresponding author on reasonable request.

Received: 19 November 2024; Accepted: 3 March 2025
Published online: 06 March 2025

References

1. Kim, J. E. et al. The effect of P2X7 receptor activation on nuclear factor-κB phosphorylation induced by status epilepticus in the rat hippocampus. *Hippocampus* **23**, 500–514. https://doi.org/10.1002/hipo.22109 (2013).
2. Feng, L. et al. P2X7R blockade prevents NLRP3 inflammasome activation and brain injury in a rat model of intracerebral hemorrhage: Involvement of peroxynitrite. *J. Neuroinflammation* **12**, 190. https://doi.org/10.1186/s12974-015-0409-2 (2015).
3. Huang, C. et al. Inhibition of P2X7 receptor ameliorates nuclear factor-kappa B mediated neuroinflammation induced by status epilepticus in rat hippocampus. *J. Mol. Neurosci.* **63**, 173–184. https://doi.org/10.1007/s12031-017-0968-z (2017).
4. Lee, D. S. & Kim, J. E. P2X7 receptor augments LPS-induced nitrosative stress by regulating Nrf2 and GSH levels in the mouse hippocampus. *Antioxidants (Basel)* **11**, 778. https://doi.org/10.3390/antiox11040778 (2022).
5. Park, H. & Kim, J. E. Deletion of P2X7 receptor decreases basal glutathione level by changing glutamate-glutamine cycle and neutral amino acid transporters. *Cells* **9**, 995. https://doi.org/10.3390/cells9040995 (2020).
6. Zai, A., Rudd, M. A., Scribner, A. W. & Loscalzo, J. Cell-surface protein disulfide isomerase catalyzes transnitrosation and regulates intracellular transfer of nitric oxide. *J. Clin. Invest.* **103**, 393–399. https://doi.org/10.1172/JCI4890 (1999).
7. Turano, C., Coppari, S., Altieri, F. & Ferraro, A. Proteins of the PDI family: Unpredicted non-ER locations and functions. *J. Cell Physiol.* **193**, 154–163. https://doi.org/10.1002/jcp.10172 (2002).
8. Ramachandran, N., Root, P., Jiang, X. M., Hogg, P. J. & Mutus, B. Mechanism of transfer of NO from extracellular S-nitrosothiols into the cytosol by cell-surface protein disulfide isomerase. *Proc. Natl. Acad. Sci. USA* **98**, 9539–9544. https://doi.org/10.1073/pnas.171180998 (2001).
9. Kim, J. Y., Ko, A. R., Hyun, H. W., Min, S. J. & Kim, J. E. PDI regulates seizure activity via NMDA receptor redox in rats. *Sci. Rep.* **7**, 42491. https://doi.org/10.1038/srep42491 (2017).
10. Lee, D. S. & Kim, J. E. PDI-mediated S-nitrosylation of DRP1 facilitates DRP1-S616 phosphorylation and mitochondrial fission in CA1 neurons. *Cell Death Dis.* **9**, 869. https://doi.org/10.1038/s41419-018-0910-5 (2018).
11. Furlan-Freguia, C., Marchese, P., Gruber, A., Ruggeri, Z. M. & Ruf, W. P2X7 receptor signaling contributes to tissue factor-dependent thrombosis in mice. *J. Clin. Invest.* **121**, 2932–2944. https://doi.org/10.1172/JCI46129 (2011).
12. Ruf, W. Role of thiol pathways in TF procoagulant regulation. *Thromb. Res.* **129**, S11-12. https://doi.org/10.1016/j.thromres.2012.02.020 (2012).
13. Lee, D. S. & Kim, J. E. Protein disulfide isomerase-mediated S-nitrosylation facilitates surface expression of P2X7 receptor following status epilepticus. *J. Neuroinflamm.* **18**, 14. https://doi.org/10.1186/s12974-020-02058-y (2021).
14. Furusawa, J. et al. Licochalcone A significantly suppresses LPS signaling pathway through the inhibition of NF-kappaB p65 phosphorylation at serine 276. *Cell Signal.* **21**, 778–785. https://doi.org/10.1016/j.cellsig.2009.01.021 (2009).
15. Gadgil, H. S. et al. Proteome of monocytes primed with lipopolysaccharide: Analysis of the abundant proteins. *Proteomics* **3**, 1767–1780. https://doi.org/10.1002/pmic.200300532 (2003).
16. Triantafyllou, E. A., Mylonis, I., Simos, G. & Paraskeva, E. Hypoxia induces pro-fibrotic and fibrosis marker genes in hepatocellular carcinoma cells independently of inflammatory stimulation and the NF-κB pathway. *Hypoxia (Auckl)* **7**, 87–91. https://doi.org/10.2147/HP.S235967 (2019).
17. Sang, A. et al. Quercetin attenuates sepsis-induced acute lung injury via suppressing oxidative stress-mediated ER stress through activation of SIRT1/AMPK pathways. *Cell Signal.* **96**, 110363. https://doi.org/10.1016/j.cellsig.2022.110363 (2022).
18. Higuchi, T., Watanabe, Y. & Waga, I. Protein disulfide isomerase suppresses the transcriptional activity of NF-kappaB. *Biochem. Biophys. Res. Commun.* **318**, 46–52. https://doi.org/10.1016/j.bbrc.2004.04.002 (2004).
19. Zhou, M. et al. Downregulation of protein disulfide isomerase in sepsis and its role in tumor necrosis factor-alpha release. *Crit. Care* **12**, R100. https://doi.org/10.1186/cc6977 (2008).
20. Xiao, Y. et al. Protein disulfide isomerase silence inhibits inflammatory functions of macrophages by suppressing reactive oxygen species and NF-κB pathway. *Inflammation* **41**, 614–625. https://doi.org/10.1007/s10753-017-0717-z (2018).
21. Wang, W. T., Sun, L. & Sun, C. H. PDIA3-regulted inflammation and oxidative stress contribute to the traumatic brain injury (TBI) in mice. *Biochem. Biophys. Res. Commun.* **518**, 657–663. https://doi.org/10.1016/j.bbrc.2019.08.100 (2019).
22. Kamarehei, M. et al. Inhibition of protein disulfide isomerase has neuroprotective effects in a mouse model of experimental autoimmune encephalomyelitis. *Int. Immunopharmacol.* **82**, 106286. https://doi.org/10.1016/j.intimp.2020.106286 (2020).
23. Matthews, J. R., Wakasugi, N., Virelizier, J. L., Yodoi, J. & Hay, R. T. Thioredoxin regulates the DNA binding activity of NF-kappa B by reduction of a disulphide bond involving cysteine 62. *Nucleic Acids Res.* **20**, 3821–3830. https://doi.org/10.1093/nar/20.15.3821 (1992).
24. Hayashi, T., Ueno, Y. & Okamoto, T. Oxidoreductive regulation of nuclear factor kappa B. Involvement of a cellular reducing catalyst thioredoxin. *J. Biol. Chem.* **268**, 11380–11388 (1993).
25. Roy, A., Fung, Y. K., Liu, X. & Pahan, K. Up-regulation of microglial CD11b expression by nitric oxide. *J. Biol. Chem.* **281**, 14971–14980. https://doi.org/10.1074/jbc.M600236200 (2006).
26. Zhong, L. M. et al. Resveratrol inhibits inflammatory responses via the mammalian target of rapamycin signaling pathway in cultured LPS-stimulated microglial cells. *PLoS ONE* **7**, e32195. https://doi.org/10.1371/journal.pone.0032195 (2012).
27. Lee, S. K., Kim, J. E., Kim, Y. J., Kim, M. J. & Kang, T. C. Hyperforin attenuates microglia activation and inhibits p65-Ser276 NFκB phosphorylation in the rat piriform cortex following status epilepticus. *Neurosci. Res.* **85**, 39–50. https://doi.org/10.1016/j.neures.2014.05.006 (2014).
28. Kim, W. I. et al. Differential nuclear factor-kappa B phosphorylation induced by lipopolysaccharide in the hippocampus of P2X7 receptor knockout mouse. *Neurol. Res.* **35**, 369–381. https://doi.org/10.1179/1743132812Y.0000000137 (2013).
29. Xie, Q. W., Kashiwabara, Y. & Nathan, C. Role of transcription factor NF-kappa B/Rel in induction of nitric oxide synthase. *J. Biol. Chem.* **269**, 4705–4708 (1994).

30. Zhao, J. et al. Neuroinflammation induced by lipopolysaccharide causes cognitive impairment in mice. *Sci. Rep.* **9**, 5790. https://doi.org/10.1038/s41598-019-42286-8 (2019).
31. Ju, C. et al. Inhibition of Dyrk1A Attenuates LPS-Induced Neuroinflammation via the TLR4/NF-κB P65 Signaling Pathway. *Inflammation* **45**, 2375–2387. https://doi.org/10.1007/s10753-022-01699-w (2022).
32. Kallakunta, V. M., Slama-Schwok, A. & Mutus, B. Protein disulfide isomerase may facilitate the efflux of nitrite derived S-nitrosothiols from red blood cells. *Redox Biol.* **1**, 373–380. https://doi.org/10.1016/j.redox.2013.07.002 (2013).
33. Kelleher, Z. T., Matsumoto, A., Stamler, J. S. & Marshall, H. E. NOS2 regulation of NF-kappaB by S-nitrosylation of p65. *J. Biol. Chem.* **42**, 30667–30672. https://doi.org/10.1074/jbc.M705929200 (2007).
34. Perkins, N. D. Cysteine 38 holds the key to NF-kappaB activation. *Mol. cell.* **1**, 1–3. https://doi.org/10.1016/j.molcel.2011.12.023 (2012).
35. Sen, N. et al. Hydrogen sulfide-linked sulfhydration of NF-κB mediates its antiapoptotic actions. *Mol. Cell.* **45**, 13–24. https://doi.org/10.1016/j.molcel.2011.10.021 (2012).
36. Kelleher, Z. T. et al. Thioredoxin-mediated denitrosylation regulates cytokine-induced nuclear factor κB (NF-κB) activation. *J. Biol. Chem.* **289**, 3066–3072. https://doi.org/10.1074/jbc.M113.503938 (2014).
37. Sudo, K., Takezawa, Y., Kohsaka, S. & Nakajima, K. Involvement of nitric oxide in the induction of interleukin-1 beta in microglia. *Brain Res.* **1625**, 121–134. https://doi.org/10.1016/j.brainres.2015.08.030 (2015).
38. Barbierato, M. et al. Astrocyte-microglia cooperation in the expression of a pro-inflammatory phenotype. *CNS Neurol. Disord. Drug Targets* **12**, 608–618. https://doi.org/10.2174/18715273113129990064 (2013).
39. Hu, Y. et al. Purinergic receptor modulation of lipopolysaccharide signaling and inducible nitric-oxide synthase expression in RAW 264.7 macrophages. *J. Biol. Chem.* **273**, 27170–27175. https://doi.org/10.1074/jbc.273.42.27170 (1998).
40. Tung, H. C. et al. The beneficial effects of P2X7 antagonism in rats with bile duct ligation-induced cirrhosis. *PLoS ONE* **10**, e0124654. https://doi.org/10.1371/journal.pone.0124654 (2015).
41. Guerra, A. N. et al. Purinergic receptor regulation of LPS-induced signaling and pathophysiology. *J. Endotoxin Res.* **9**, 256–263. https://doi.org/10.1179/096805103225001468 (2003).
42. Friedle, S. A., Brautigam, V. M., Nikodemova, M., Wright, M. L. & Watters, J. J. The P2X7-Egr pathway regulates nucleotide-dependent inflammatory gene expression in microglia. *Glia* **59**, 1–13. https://doi.org/10.1002/glia.21071 (2011).
43. Dang, R. et al. Fish oil supplementation attenuates neuroinflammation and alleviates depressive-like behavior in rats submitted to repeated lipopolysaccharide. *Eur. J. Nutr.* **57**, 893–906. https://doi.org/10.1007/s00394-016-1373-z (2018).
44. Walker, A. K. et al. Protein disulphide isomerase protects against protein aggregation and is S-nitrosylated in amyotrophic lateral sclerosis. *Brain* **133**, 105–116. https://doi.org/10.1093/brain/awp267 (2010).
45. Wang, H., Wang, P. & Zhu, B. T. Mechanism of erastin-induced ferroptosis in MDA-MB-231 human breast cancer cells: Evidence for a critical role of protein disulfide isomerase. *Mol. Cell Biol.* **42**, e0052221. https://doi.org/10.1128/mcb.00522-21 (2022).
46. Akagi, S. et al. Distribution of protein disulfide isomerase in rat hepatocytes. *J. Histochem. Cytochem.* **36**, 1533–1542. https://doi.org/10.1177/36.12.3192937 (1988).
47. Rigobello, M. P., Donella-Deana, A., Cesaro, L. & Bindoli, A. Distribution of protein disulphide isomerase in rat liver mitochondria. *Biochem. J.* **356**, 567–570. https://doi.org/10.1042/0264-6021:3560567 (2001).
48. Kawahara, K. et al. Induction of CHOP and apoptosis by nitric oxide in p53-deficient microglial cells. *FEBS. Lett.* **506**, 135–139. https://doi.org/10.1016/s0014-5793(01)02898-8 (2001).
49. Tanaka, S., Uehara, T. & Nomura, Y. Up-regulation of protein-disulfide isomerase in response to hypoxia/brain ischemia and its protective effect against apoptotic cell death. *J. Biol. Chem.* **275**, 10388–10393. https://doi.org/10.1074/jbc.275.14.10388 (2000).
50. Hashemy, S. I. & Holmgren, A. Regulation of the catalytic activity and structure of human thioredoxin 1 via oxidation and S-nitrosylation of cysteine residues. *J. Biol. Chem.* **283**, 21890–21898. https://doi.org/10.1074/jbc.M801047200 (2008).
51. Aga, M. et al. Evidence for nucleotide receptor modulation of cross talk between MAP kinase and NF-kappa B signaling pathways in murine RAW 264.7 macrophages. *Am. J. Physiol Cell Physiol.* **286**, C923–C930. https://doi.org/10.1152/ajpcell.00417.2003 (2004).
52. Coddou, C., Yan, Z., Obsil, T., Huidobro-Toro, J. P. & Stojilkovic, S. S. Activation and regulation of purinergic P2X receptor channels. *Pharmacol. Rev.* **63**, 641–683. https://doi.org/10.1124/pr.110.003129 (2011).
53. Jindrichova, M., Kuzyk, P., Li, S., Stojilkovic, S. S. & Zemkova, H. Conserved ectodomain cysteines are essential for rat P2X7 receptor trafficking. *Purinergic Signal.* **8**, 317–325. https://doi.org/10.1007/s11302-012-9291-x (2012).
54. Lipton, S. A. et al. Cysteine regulation of protein function–as exemplified by NMDA-receptor modulation. *Trends Neurosci.* **25**, 474–480. https://doi.org/10.1016/s0166-2236(02)02245-2 (2002).
55. Sekar, P., Huang, D. Y., Hsieh, S. L., Chang, S. F. & Lin, W. W. AMPK-dependent and independent actions of P2X7 in regulation of mitochondrial and lysosomal functions in microglia. *Cell Commun. Signal.* **16**, 83. https://doi.org/10.1186/s12964-018-0293-3 (2018).
56. Bockstiegel, J., Engelhardt, J. & Weindl, G. P2X7 receptor activation leads to NLRP3-independent IL-1β release by human macrophages. *Cell Commun. Signal.* **21**, 335. https://doi.org/10.1186/s12964-023-01356-1 (2023).
57. Balboa, M. A., Balsinde, J., Johnson, C. A. & Dennis, E. A. Regulation of arachidonic acid mobilization in lipopolysaccharide-activated P388D(1) macrophages by adenosine triphosphate. *J. Biol. Chem.* **274**, 36764–36768. https://doi.org/10.1074/jbc.274.51.36764 (1999).
58. Lee, D. S., Kim, T. H., Park, H. & Kim, J. E. PDI augments kainic acid-induced seizure activity and neuronal death by inhibiting PP2A-GluA2-PICK1-mediated AMPA receptor internalization in the mouse hippocampus. *Sci. Rep.* **13**, 13927. https://doi.org/10.1038/s41598-023-41014-7 (2023).

Acknowledgements

This study was supported by a grant of National Research Foundation of Korea (NRF) grant (No. 2021R1A2C4002003). The funders had no role in study design, data collection and analysis, decision to publish, or preparation of the manuscript.

Author contributions

J-EK designed and supervised the project. D-SL, T-HK and SYW performed the experiments described in the manuscript with J-EK and analyzed the data. J-EK wrote the manuscript.

Declarations

Competing interests

The authors declare no competing interests.

Ethics approval and consent to participate

Animal protocols were approved by the Institutional Animal Care and Use Committee of Hallym University, Chuncheon, South Korea, Code number: (#Hallym 2021-30, approval date: May 17, 2021).

Additional information

Supplementary Information The online version contains supplementary material available at https://doi.org/10.1038/s41598-025-92780-5.

Correspondence and requests for materials should be addressed to J.-E.K.

Reprints and permissions information is available at www.nature.com/reprints.

Publisher's note Springer Nature remains neutral with regard to jurisdictional claims in published maps and institutional affiliations.